Charged particle trajectories in an ideal paracentric hemispherical deflection analyzer

T. J. M. Zouros, E. P. Benis, and J. E. Schauer

Charged particle trajectories in an ideal paracentric hemispherical deflection analyser

T. J. M. Zouros,[*a,b] E. P. Benis[a,b] and J.E. Schauer[a,c]

[a]Dept. of Physics, University of Crete, P.O. Box 2208, 71003 Heraklion, Crete
[b]Institute of Electronic Structure and Laser, FORTH, Heraklion, Crete, GREECE
[c]Dept. of Physics, Concordia College, Moorhead, Minnesota, 56562, USA

Abstract. We present an exact analytic solution for the trajectory of a charged particle moving in the ideal potential $\tilde{V}(r) = -k/r + c$ inside a hemispherical deflector analyser (HDA). Our treatment extends the known solutions to also include paracentric entry for which $R_0 \neq \bar{R} \equiv \frac{1}{2}(R_1 + R_2)$ and $\tilde{V}(R_0)$ is <u>not</u> necessarily zero, where R_0 is the centre of the HDA entry aperture. We also account for particle refraction at the potential boundary that cannot be neglected when $\tilde{V}(R_0) \neq 0$. A general 3-D vector treatment for calculating trajectories in a fixed frame is also described based on the conservation of the angular momentum and eccentricity vectors. These results find applications in modern hemispherical spectrographs incorporating large diameter position sensitive detectors (PSD) as for example in ESCA.

INTRODUCTION

Recently, we have reported on the use of a *paracentric* HDA with 2-D PSD (1) for high-resolution zero-degree Auger projectile electron spectroscopy. (2) A *paracentric* HDA has an *elliptical* central trajectory with particle entry at $R_0 < \bar{R} \equiv \frac{1}{2}(R_1 + R_2)$ and $\tilde{V}_0 \equiv \tilde{V}(R_0) \neq 0$, (1) unlike a *conventional* HDA having a *circular* central trajectory with $R_0 = \bar{R}$ and $\tilde{V}_0 = 0$. A typical paracentric HDA geometry is shown in Fig. 1.

The paracentric HDA has been shown (1) using charged particle optics program SIMION3D (3) to have superior energy resolution and larger acceptance energy window than that of a conventional HDA *without* the use of fringing field correctors. (4) The reason for this is not yet clear. By computing the 3-D trajectories of particles in an ideal and a <u>real</u> (simulated by SIMION) paracentric analyser we expect to get a better understanding of the specific ways by which fringing field effects modify the behavior of such analysers.

Paracentric HDAs have never been treated in the literature. However, very recently, a high-resolution tandem energy analyser incorporating an exit paracentric HDA (i.e. $R_0 = \bar{R}$ but $R_\pi < \bar{R}$) as the second stage has been briefly described.(5) We expect our general approach to be of particular interest to investigators using modern HDAs (for a recent review see (6)) with substantial interradial distances needed to accommodate

large area PSDs (7) or second stages (8, 9) in which fringing fields (4, 10) and refraction at field boundaries
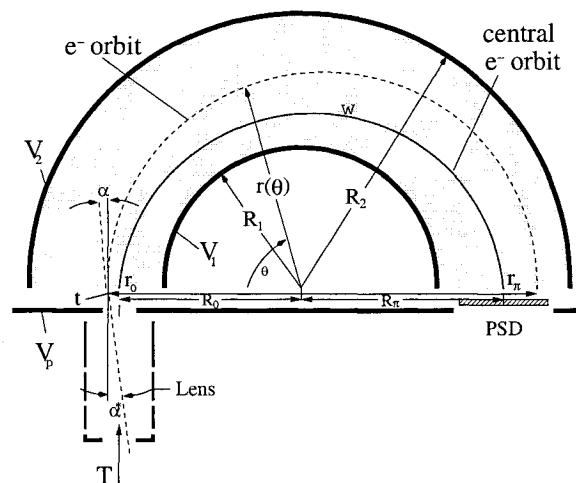
FIGURE 1. Schematic of paracentric HDA geometry. The charged particle initially enters the lens assembly with kinetic energy T and is then focused and decelerated by the lens and plate at potential V_p down to an energy t just prior to entering the interior region of the analyser (shaded area) with angle $\alpha^\star$. Upon entering at r_0 at potential $V(r_0)$, it is refracted to an angle α, follows the trajectory specified by $r(\theta)$ and exits at r_π after being deflected through an angle π. The centre of the entrance aperture is paracentric at $R_0 < \bar{R}$. Fixing the central trajectory ($\alpha = 0$) such that for $t = w$ and $r_0 = R_0$, $r_\pi = R_\pi$ fixes the analyser voltages.

* Corresponding author - tzouros@physics.uoc.gr

(8, 9) are important and may be used to advantage.(11) This is a work in progress and here we briefly present some of our first analytic results.

TRAJECTORY EQUATIONS

The classical, non-relativistic equations of motion for a particle of mass m and charge q in the potential $\tilde{V}(r)$ are given by:

$$m\ddot{\mathbf{r}} + q\,\boldsymbol{\nabla}\tilde{V}(r) = 0 \qquad (1)$$

For the solution of $\mathbf{r}$ *inside* an ideal HDA we use $\tilde{V}(r) = -\frac{k}{r} + c$. The eccentricity vector $\boldsymbol{\epsilon}$ is given by:(12)

$$\boldsymbol{\epsilon} \equiv \frac{\dot{\mathbf{r}} \times \mathbf{L}}{qk} - \frac{\mathbf{r}}{r} \qquad (2)$$

It is seen to be proportional to the Runge-Lenz vector $\mathbf{A} = qk\boldsymbol{\epsilon}$ (13) known to be *conserved* for motion in a $1/r$ potential. Clearly, $\boldsymbol{\epsilon}$ lies in the orbital plane since from Eq. 2 it is seen to be perpendicular to the angular momentum $\mathbf{L}$.

Taking the dot product of $m\mathbf{r}$ with Eq. 2 yields the scalar equation of motion for r:

$$r(\theta) \equiv r_\theta = r = \frac{p}{1 + \hat{\mathbf{r}} \cdot \boldsymbol{\epsilon}} = \frac{p}{1 + \epsilon\cos(\theta - \theta_\epsilon)} \qquad (3)$$

Eq. 3 is seen to be the equation of a conic section in polar coordinates with the origin of the coordinate frame at the focus of the conic section. For $0 < \epsilon < 1$, the orbit is an ellipse with eccentricity $\epsilon = |\boldsymbol{\epsilon}|$ and *latus rectum* $p = L^2/(m\,q\,k)$ (13) with $L = mr_0v_0\cos\alpha$. The angle $\theta - \theta_\epsilon$ is just the angle between the two vectors $\mathbf{r}$ and $\boldsymbol{\epsilon}$. At entry, we have $\theta = \theta_0$ and $r_0 \equiv r(\theta = \theta_0)$. When $\theta = \theta_\epsilon$, it is seen that r is a minimum and thus $\boldsymbol{\epsilon}$ has the useful property that it *always points to periapse*.

Using Eq. 3 and specifying the *central* trajectory such that a particle with kinetic energy $t = w$ just prior to entry with $\alpha = 0$ and $r_0 = R_0$, exits at $r_\pi = R_\pi$, necessarily sets the values for $\tilde{V}(r)$ constants k and c:

$$qk = \gamma w R_0 \left(1 + \frac{R_0}{R_\pi}\right) \qquad qc = w\left(1 + \gamma\frac{R_0}{R_\pi}\right) \quad (4)$$

where we have also defined $q\tilde{V}_0 \equiv (1 - \gamma)w$ with γ a control parameter used to set the voltages of the HDA.

i. $\theta_\epsilon = 0$ vector form of the orbit

Clearly, the conserved vectors $\boldsymbol{\epsilon}$ and $\mathbf{L} \times \boldsymbol{\epsilon}$ are mutually perpendicular to $\mathbf{L}$ and therefore lie in the plane of the orbit. They can be used as a natural coordinate system of axes to describe the motion. Choosing to align the x-axis along the semi-major axis ($\theta_\epsilon = 0$) we may set: (14)

$$\mathbf{r}(t) = x(t)\frac{\boldsymbol{\epsilon}}{\epsilon} + y(t)\frac{\mathbf{L} \times \boldsymbol{\epsilon}}{L\epsilon} \qquad (5)$$

with the focus of the ellipse (see Fig. 2) at $r = 0$ and (13)

$$x(t) = a(\cos\zeta - \epsilon) \qquad (6)$$

$$y(t) = a\sqrt{(1 - \epsilon^2)}\sin\zeta \qquad (7)$$

$$t = \sqrt{\frac{m\,a^3}{q\,k}}(\zeta - \epsilon\sin\zeta) \qquad (8)$$

with the particle being at periapse at time $t = 0$ and $\zeta = \theta = 0$. The semi-major axis of the ellipse has length $a = (r_0 + r_\pi)/2 = p/(1 - \epsilon^2)$ obtained directly from Eq 3.

The new angle ζ introduced above is known as the Kepler (14) or eccentric anomaly (12) and is related to the angle θ by:

$$\tan\frac{\zeta}{2} = \sqrt{\frac{1 - \epsilon}{1 + \epsilon}}\tan\frac{\theta}{2} \qquad (9)$$

Eq. 9 is particularly useful as it avoids quadrant ambiguity since $\zeta/2$ is always in the same quadrant as $\theta/2$ (12). Using Eq. 5 it is straightforward to describe the 3-D tra-
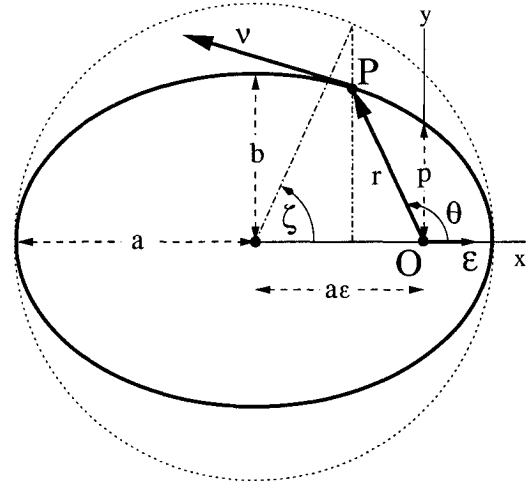
FIGURE 2. Elliptical particle orbit in the xy coordinate system showing the *true anomaly* θ and the *eccentric anomaly* ζ and *latus rectum p*. O is the center of attraction and focus of the ellipse. The eccentricity vector $\boldsymbol{\epsilon}$ is seen to start from O and point to periapse. It thus *always lies along the semimajor axis* of the ellipse.

jectory in any fixed coordinate system XYZ in which the initial components of $\mathbf{L}$ and $\boldsymbol{\epsilon}$ are known. In Fig. 3 we show such a 3-D plot made with the help of the software program *Mathematica*.

Eq. 8 is also very useful since it gives directly the time-of-flight (TOF) as a function of the eccentric anomaly ζ. Thus, for a particle entering the HDA at t = t_0 with θ_0, r_0 and v_0 and exiting after a deflection by π we have:

$$\text{TOF} = \sqrt{\frac{m\,a^3}{q\,k}}[\zeta_\pi - \zeta_0 - \epsilon(\sin\zeta_\pi - \sin\zeta_0)] \quad (10)$$
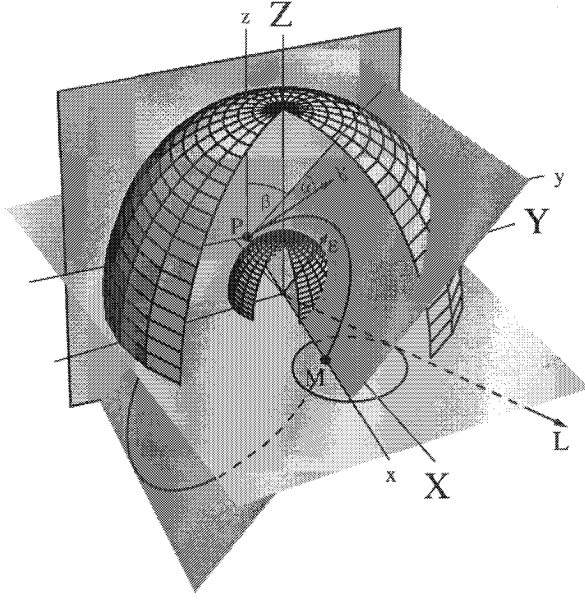
FIGURE 3. 3-D orbit in HDA: Charged particle enters at P and exits at M with $\alpha = -30°$, $\beta = -50°$, $\gamma = 1.5$, $\tau = 1.16$ and $w = 1000$ eV. **XYZ** is the fixed laboratory frame, while xyz is the relative reference frame traditionally used to describe the orbit in terms of angles α and β. The entry velocity $\mathbf{v}_0$, eccentricity ϵ and angular momentum **L** are also shown.

where $\zeta_0 \equiv \zeta(\theta_0)$ and $\zeta_\pi \equiv \zeta(\theta_0 + \pi)$. The orbit angle θ_0 is determined from Eq. 3 with $r = r_0$, $\theta = \theta_0$ and $\theta_\epsilon = 0$.

ii. $\theta_0 = 0$ scalar form of the orbit

Another useful form of the radial equation Eq. 3 is obtained by orienting our xy coordinate system so that $\mathbf{r}_0$ lies along the positive x-axis (i.e. $\theta_0 = 0$):

$$\frac{r_0}{r_\theta} = \frac{q\,k}{m\,v_0^2\,r_0}\frac{(1 - \cos\theta)}{\cos^2\alpha} + \cos\theta - \tan\alpha\sin\theta \quad (11)$$

where we have also used the initial condition $\dot{r}_0 = v_0\sin\alpha = -\frac{L}{m\,p}\epsilon\sin\theta_\epsilon$ obtained by evaluating $\dot{r}$ directly from Eq. 3 at entry. Eq. 11 is the well-known form introduced by Purcel (15) and discussed in more detail in Refs. (16, 17, 18, 7, 10). Eq. 11 also exhibits the well-known double focusing properties of the HDA, since for $\theta = \pi$ it is clear that $\partial r_\theta / \partial\alpha = 0$ at $\alpha = 0$. However, it does not include corrections for refraction discussed next.

REFRACTION CORRECTIONS

So far we have derived the trajectories in terms of initial conditions *within* the field of the analyser. However, right outside the analyser (just before entry) the potential

is constant and thus changes discontinuously across the boundary at θ_0 (at the border of the shaded area in Fig. 1). This discontinuity can be represented mathematically by defining the step potential $\tilde{V}(r,\theta)$ in the orbital plane as:

$$\tilde{V}(r,\theta) = \tilde{V}(r)\,u(\theta - \theta_0) \quad (12)$$

where $u(\theta - \theta_0)$ is the unit step function.

It can be easily shown that the energy is conserved in going across the potential step and thus:

$$\Delta K^\star \equiv \frac{1}{2}mv_0^2 - \frac{1}{2}mv_0^{\star2} = \frac{1}{2}mv_0^2 - t = -q\,\tilde{V}(r_0) \quad (13)$$

Furthermore, using the step potential $\tilde{V}(r,\theta)$ in the equation of motion for the θ coordinate we can show that:

$$\frac{dL}{dt} = -q\,\tilde{V}(r)\delta(\theta - \theta_0) \quad (14)$$

where $\delta(\theta - \theta_0) = d\,u(\theta - \theta_0)/d\theta$ is the Dirac delta-function. After replacing d/dt with $\dot{\theta}d/d\theta$ we obtain:

$$\frac{d}{d\theta}(L^2) = -2\,m\,r^2\,q\,\tilde{V}(r)\delta(\theta - \theta_0) \quad (15)$$

with $L = m\,r^2\,\dot{\theta}$. Upon integrating across the boundary $\theta = \theta_0$ along a path of constant $r = r_0$ we obtain:

$$L^2 - L^{\star2} = -2\,m\,r_0^2\,q\,\tilde{V}(r_0) \quad (16)$$

where the $\star$ tags parameters on the side where the particle is free. Thus, outside the analyser $L^\star = m\,r_0\,v_0^\star\,\cos\alpha^\star$, and inside the analyser $L = m\,r_0\,v_0\cos\alpha$ where v_0, $v_0^\star$ and α, $\alpha^\star$ are the velocities and entry angles inside and outside the analyser, respectively. Using Eqs. 13 and 16 above it is straightforward to derive the law of refraction for charged particles, analogous to Snell's law for light:

$$v_{r_0}^\star = v_0^\star\sin\alpha^\star = v_0\sin\alpha = v_{r_0} \quad (17)$$

or

$$\sin\alpha = \frac{\sin\alpha^\star}{\sqrt{1 + \frac{\Delta K^\star}{t}}} \quad (18)$$

From Eq. 17 it is seen that the radial velocity, $v_r = \dot{r}$, is continuous across the potential boundary(7), as opposed to the angular velocity, $v_\theta = \frac{L}{m\,r}$ which is not. The effect of refraction is shown in Fig. 4. The discontinuity effects across the sharp potential boundary at $\theta = \theta_0$, have not been given sufficient attention, especially in older publications, leading to some confusion in the literature. This has been primarily due to the fact that in *conventional* HDAs, the entry voltage $\tilde{V}_0 = 0$ and the entry slits are very narrow so that the approximation $\tilde{V}(r_0) \approx \tilde{V}_0 = 0$ is valid. Correct formuli for refraction can be found in Refs. (15, 19, 7, 8, 9).
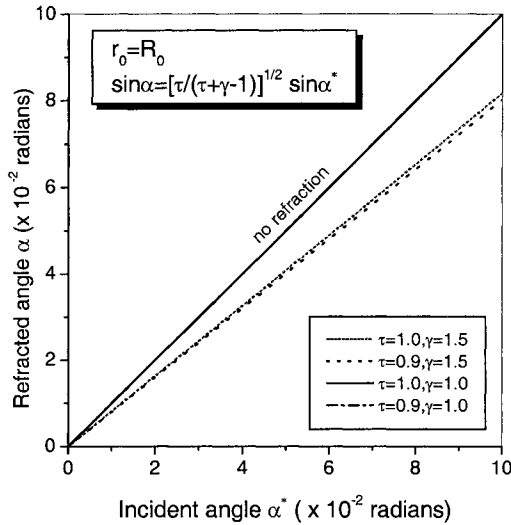
FIGURE 4. Relation between the entry angle $\alpha^\star$ prior to refraction (angle of incidence) and angle α after refraction (angle of refraction) for two cases: (a) $\tilde{V}_0 = 0$ ($\gamma = 1$), $R_0 = \bar{R}$, (b) $\tilde{V}_0 = 0.5w$ ($\gamma = 1.5$), $R_0 = 0.8125\bar{R}$ (paracentric entry). w is the energy of the central trajectory or "tuning" energy of the HDA. In both cases, $w = 1000$ eV, $r_0 = R_0$ and $R_\pi = \bar{R}$. Clearly, the effect of refraction is non-negligible for paracentric entry and $\tilde{V}_0 \neq 0$ ($\gamma \neq 1$).

Using Eqs. 13, 16 and 18 we obtain the trajectory equation in terms of the entry angle $\alpha^\star$ and velocity $v_0^\star$:

$$\frac{r_0}{r_\theta} = \frac{q\,k}{m\,v_0^{\star 2}\,r_0}\frac{(1-\cos\theta)}{(1+\frac{\Delta K^\star}{t\cos^2\alpha^\star})\cos^2\alpha^\star}$$
$$+ \cos\theta - \frac{\tan\alpha^\star\,\sin\theta}{\sqrt{1+\frac{\Delta K^\star}{t\cos^2\alpha^\star}}} \qquad (19)$$

where we have also introduced the reduced pass energy $\tau \equiv t/w$. Clearly, Eq. 19 also preserves the first-order focusing in $\alpha^\star$ for $\theta = \pi$. Thus, following deflection by $180°$ and using Eq. 4 to rewrite potential constants k and c in terms of γ and the tuning energy w, the exit radial position r_π is given by the simple formula:

$$r_\pi = -r_0 + \frac{R_0 + R_\pi}{1 + \frac{R_\pi}{R_0\gamma}(1 - \tau\cos^2\alpha^\star)} \qquad (20)$$

Eq. 20 is thus seen to extend the well known results for the exit point of a conventional HDA with $R_0 = R_\pi = \bar{R}$ and $\tilde{V}_0 = 0$ (e.g. see (7)) to those of the more general paracentric case, where $R_0 \neq R_\pi \neq \bar{R}$ and where $\tilde{V}_0$ might also be different from zero. The optical properties of the HDA (e.g. resolution, transmission, etc.) directly follow from Eq. 20 and are presented elsewhere (20).

REFERENCES

1. E. P. Benis and T. J. M. Zouros, Nucl. Instrum. Methods Phys. Res. Sect. A **440**, 462 (2000).
2. T. J. M. Zouros and D. H. Lee, in *Accelerator-based atomic physics techniques and applications*, edited by S. M. Shafroth and J. C. Austin (American Institute of Physics Conference Series, New York, 1997), pp. 426–79.
3. D. A. Dahl, SIMION 3D v6.0, Idaho National Engineering Laboratory, Idaho Falls 1996.
4. D. Hu and K. Leung, Rev. Sci. Instrum. **66**, 2865 (1995) and references therein.
5. V. D. Belov and M. I. Yavor, Rev. Sci. Instrum. **71**, 1651 (2000).
6. D. Roy and D. Tremblay, Rep. Prog. Phys. **53**, 1621 (1990).
7. F. Hadjarab and J. Erskine, J. Electr. Spectr. and Rel. Phenom. **36**, 227 (1985).
8. A. Mann and F. Linder, J. Phys. E: Sci. Instrum. **21**, 805 (1988).
9. A. Baraldi and V. R. Dhanak, J. Electr. Spectr. and Rel. Phenom. **67**, 211 (1994).
10. P. Louette *et al.*, J. Electr. Spectr. and Rel. Phenom. **52**, 867 (1990).
11. S. C. Page and F. H. Read, Nucl. Instrum. Methods Phys. Res. Sect. A **363**, 249 (1995).
12. J. E. Prussing and B. A. Conway, *Orbital Mechanics* (Oxford University Press, Oxford, 1993).
13. D. L. Landau and E. M. Lifschitz, *Mechanics* (2nd edition Pergamon Press, Addison-Wesley Publishing Company, Inc., Reading, Massachusetts, 1969).
14. E. A. Solov'ev, Sov. Phys. JETP **55**, 1017 (1982).
15. E. Purcell, Phys. Rev. **54**, 818 (1938).
16. H. Wollnik, Nucl. Instr. & Meth. **34**, 213 (1965).
17. D. Roy and J.-D. Carette, Canadian J. of Phys. **49**, 2138 (1971).
18. M. E. Rudd, in *Low Energy Electron Spectrometry*, edited by K. D. Sevier (Wiley, New York, 1972), pp. 17–34.
19. R. E. Imhof, A. Adams, and G. King, J. Phys. E: Sci. Instrum. **9**, 138 (1976).
20. E. P. Benis and T. J. M. Zouros, Dept. of Physics, Univ. of Crete, internal report and to be published.